

# Effects of Salinity and the Extent of Water on Supercritical CO<sub>2</sub>-Induced Phlogopite Dissolution and Secondary Mineral Formation

Hongbo Shao, Jessica R. Ray, and Young-Shin Jun\*

Department of Energy, Environmental and Chemical Engineering, Washington University in St. Louis, St. Louis, Missouri 63130, United States

**S** Supporting Information

**ABSTRACT:** To ensure the viability of geologic CO<sub>2</sub> sequestration (GCS), we need a holistic understanding of reactions at supercritical CO<sub>2</sub> (scCO<sub>2</sub>)-saline water-rock interfaces and the environmental factors affecting these interactions. This research investigated the effects of salinity and the extent of water on the dissolution and surface morphological changes of phlogopite [KMg<sub>2.87</sub>Si<sub>3.07</sub>Al<sub>1.23</sub>O<sub>10</sub>(F,OH)<sub>2</sub>], a model clay mineral in potential GCS sites. Salinity enhanced the dissolution of phlogopite and affected the location, shape, size, and phase of secondary minerals. In low salinity solutions, nanoscale particles of secondary minerals formed much faster, and there were more nanoparticles than in high salinity solutions. The effect of water extent was investigated by comparing scCO<sub>2</sub>-H<sub>2</sub>O(g)-phlogopite and scCO<sub>2</sub>-H<sub>2</sub>O(l)-phlogopite interactions. Experimental results suggested that the presence of a thin water film adsorbed on the phlogopite surface caused the formation of dissolution pits and a surface coating of secondary mineral phases that could change the physical properties of rocks. These results provide new information for understanding reactions at scCO<sub>2</sub>-saline water-rock interfaces in deep saline aquifers and will help design secure and environmentally sustainable CO<sub>2</sub> sequestration projects.

## INTRODUCTION

Carbon dioxide sequestration in deep saline formations is an attractive option among geologic CO<sub>2</sub> sequestration (GCS) strategies.<sup>1,2</sup> However, dissolution of rocks and secondary mineral formation induced by CO<sub>2</sub> injection (Figure 1) could potentially change the physical properties of the geological formations and thus influence the transport and injectivity of CO<sub>2</sub>.<sup>3,4</sup> Although the injection phase of GCS could last as long as 25 years or more,<sup>3</sup> recent studies have shown that supercritical CO<sub>2</sub> (scCO<sub>2</sub>)-induced dissolution and precipitation can change the rock's porosity and permeability after a short time.<sup>5,6</sup> For example, in our previous study, nanoscale precipitates appeared on phlogopite surfaces after only 5 h reaction under simulated GCS conditions.<sup>6</sup> Therefore, experimental studies on mineral-fluid (scCO<sub>2</sub> and saline water) interactions for short time scales are important to achieve better predictions of the short- and long-term risks associated with GCS.

Salinity is one of the many environmental parameters that can influence reactions among scCO<sub>2</sub>, water, and rocks.<sup>3,4,7</sup> The salinity of brine in geologic formations can vary between several mg/L to several hundred g/L.<sup>8,9</sup> For example, in the Michigan basin, USA, the salinity is over 400 000 mg/L, whereas at Silurian, Indiana, USA, a salinity of 500 mg/L was reported.<sup>8</sup> Moreover, salinity in sedimentary basins generally increases with depth, but the rate of increase varies at different locations.<sup>9</sup> Therefore, for different GCS sites, the salinity could vary significantly. The effects of salinity on the dissolution of rock minerals are not well understood yet, and most studies have been conducted in acid solution without the presence of scCO<sub>2</sub><sup>7,10</sup> (and references therein). For example, in acid solutions without scCO<sub>2</sub>, the dissolution rates of feldspars were significantly decreased by an

increase of salinity at pH 3 at 25 °C,<sup>11</sup> whereas the dissolution of forsterite (Mg<sub>2</sub>SiO<sub>4</sub>) was not influenced by ionic strength for salinity up to 12 mol/kg over a pH range of 1–4 at 25 °C.<sup>7</sup> So far, there is no report on the effect of salinity on the dissolution and surface morphology changes of clay minerals under GCS conditions.

Aqueous-phase-mediated chemical reactions with dissolved CO<sub>2</sub> have been considered the principal process for interactions between CO<sub>2</sub> and rocks in GCS systems. However, for GCS, chemical interactions are also possible between water vapor coexisting in the scCO<sub>2</sub>-rich phase (referred as scCO<sub>2</sub>-H<sub>2</sub>O(g) hereafter) and rocks and between pure scCO<sub>2</sub> and rocks.<sup>3</sup> The latter is less likely because the abundant water in deep saline aquifers will allow a small extent of water (water vapor) to enter the scCO<sub>2</sub> phase soon after CO<sub>2</sub> injection.<sup>12</sup> Due to the buoyancy of scCO<sub>2</sub>, the interactions between scCO<sub>2</sub>-H<sub>2</sub>O(g) and rocks mainly occur at the upper portion of formation rocks and the lower level of caprocks (regime A in Figure 1). McGrail et al. reported that the small amount of water vapor in scCO<sub>2</sub> is quite reactive toward both steel and silicate mineral surfaces under simulated GCS conditions.<sup>13</sup> However, experimental data are still very limited in this regime.<sup>3</sup> The latter is less likely because the abundant water in deep saline aquifers will allow a small extent of water (water vapor) to enter the scCO<sub>2</sub> phase soon after CO<sub>2</sub> injection.<sup>12</sup>

**Received:** October 25, 2010

**Accepted:** December 28, 2010

**Revised:** December 24, 2010

**Published:** January 11, 2011

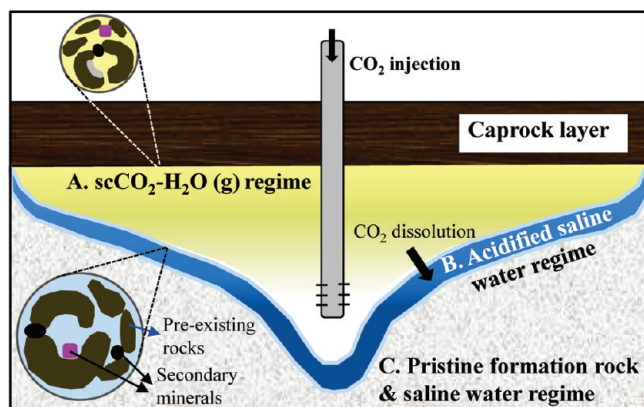


**Figure 1.** Schematic diagram of potential  $\text{CO}_2$ -saline water-rock interactions in GCS sites.

The objectives of this research were to investigate the effects of salinity and the extent of water on physical properties of rocks under GCS conditions and to relate these two parameters to the operation of GCS projects. Specifically, this study aimed to understand the surface morphology change and/or dissolution kinetics of phlogopite in three systems under 102 atm and 368 K:  $\text{scCO}_2$ -1 M NaCl,  $\text{scCO}_2$ - $\text{H}_2\text{O}(\text{l})$ , and  $\text{scCO}_2$ - $\text{H}_2\text{O}(\text{g})$ . Phlogopite, a Mg-end member mica, was used in this work as a model clay mineral because mica has been found to be widely present in GCS sites.<sup>6,14</sup> Using both fluid chemistry and surface analysis techniques, this work provides new and unique quantitative and qualitative information on nanoscale multiphase fluid-rock interactions under GCS conditions.

## EXPERIMENTAL SECTION

**Chemicals and Minerals.** All chemicals used in this study were at least ACS grade. Deionized water was passed through two 0.2  $\mu\text{m}$  filters before use. Phlogopite [formula:  $\text{KMg}_{2.87}\text{Si}_{3.07}\text{Al}_{1.23}\text{O}_{10}(\text{F},\text{OH})_2$ , based on sample characterization from our previous work<sup>6</sup>] was obtained from Ward's Natural Science, NY. Phlogopite specimens were cleaved to thin samples ( $\sim 20$   $\mu\text{m}$ , {001} cleavage surface), cut into rectangular flakes with dimensions of 2.5 cm  $\times$  0.8 cm, and cleaned.<sup>6</sup> Phlogopite powder was prepared by grinding cleaned flakes and passing the powder through a 90  $\mu\text{m}$  sieve. Powder samples were used only for secondary mineral identification.

**High Pressure/Temperature Reaction System and Dissolution Experiments.** A high P/T reactor (300 mL, Parr Instrument Company, IL) was used to study the interactions between  $\text{scCO}_2$  and phlogopite.<sup>6</sup> A phlogopite flake and 4 mL of water or 1 M NaCl was put in several PTFE tubes (the liquid/solid ratio was 400:1 by weight) in the reactor before  $\text{CO}_2$  was injected, and the pressure and temperature were controlled to be 102 atm and 368 K, respectively. Although only water was added to the  $\text{scCO}_2$ - $\text{H}_2\text{O}(\text{l})$ -phlogopite system, due to phlogopite dissolution, the aqueous solution had slight salinity (less than 50 mg/L, based on the experimentally measured aqueous concentrations (Figure 2)). For some experiments, 30 mL water was added in the reactor outside the test tubes which contained only a phlogopite flake but no water. In these experiments, the phlogopite flakes in the test tubes were actually in contact with  $\text{scCO}_2$  saturated with water vapor ( $\text{scCO}_2$ - $\text{H}_2\text{O}(\text{g})$ ). Under our experimental conditions (102 atm and 368 K), the fugacity of water vapor in  $\text{scCO}_2$  is estimated to be around 1.5 atm.<sup>12</sup> The

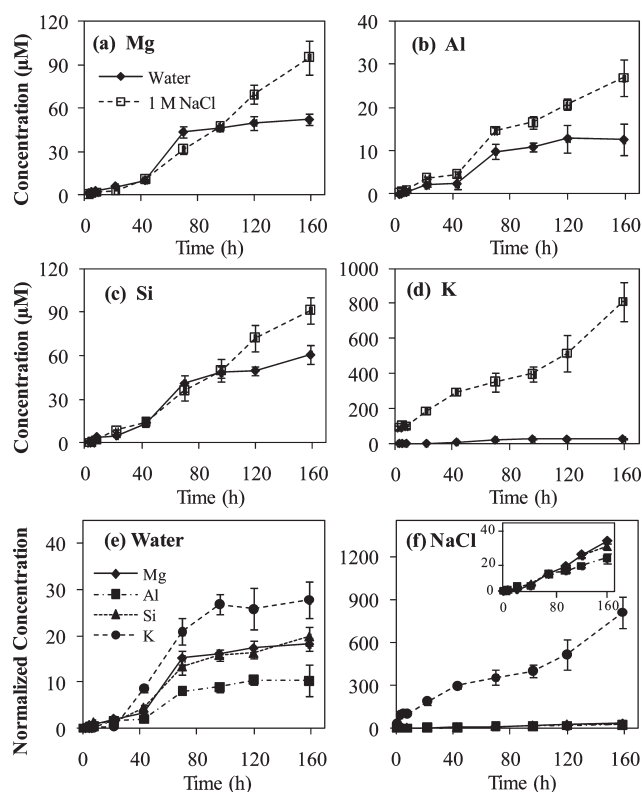


**Figure 2.** Dissolution of Mg (a), Al (b), Si (c), and K (d) from phlogopite in water and in 1 M NaCl at 102 atm and 368 K. In e and f the concentrations are normalized with the stoichiometry of the phlogopite formula  $[\text{KMg}_{2.87}\text{Si}_{3.07}\text{Al}_{1.23}\text{O}_{10}(\text{F},\text{OH})_2]$ . The inset in f is an enlarged figure for Si, Mg, and Al in 1 M NaCl solution. Error bars correspond to the standard deviation of the means of three measurements for triplicate samples.

pressure, temperature, and salinity were chosen because they are relevant to GCS conditions based on reported parameters for GCS sites,<sup>1-4,8,9</sup> and they allow obtaining experimental results within a reasonable time period. Separate reactor runs were made for each of the desired elapsed times (3, 5, 8, 22, 43, 70, 96, 120, and 159 h), after which the liquid samples were analyzed with an inductively coupled plasma-mass spectrometer (ICP-MS) (7500ce, Agilent Technologies, Santa Clara, CA). The phlogopite samples were washed with water and dried under high purity  $\text{N}_2$  to measure the surface morphology with AFM (Nanoscope V Multimode SPM, Veeco). The in situ pH of the reaction system with the same liquid/solid ratio for phlogopite flakes was measured as described previously.<sup>6</sup>

**Identification of Secondary Mineral Phases.** Because the identity of nanoscale secondary minerals on phlogopite flakes was not able to be detected due to their small quantity (for more detailed information, refer to ref 6), we conducted experiments with phlogopite powder to facilitate the formation of secondary minerals. Phlogopite powder (0.4 g) was added to test tubes containing 4 mL water or 1 M NaCl (the liquid/solid ratio was 10:1 by weight) or no water/solution at all. After reaction (159 h), the solid phase separated by centrifuging was dried and analyzed with diffuse reflectance infrared Fourier transform spectroscopy (DRIFTS, Thermo Scientific, Nicolet Nexus 470) and synchrotron-based high-resolution X-ray diffraction (HR-XRD) at the Advanced Photon Source. The supernatant was analyzed with high resolution transmission electron

microscopy (HR-TEM, JEOL JEM-2100F field emission). One caveat of this experimental approach, however, is that the products from phlogopite powder might be different from those observed in AFM images for phlogopite flake samples.

## RESULTS AND DISCUSSION

**Effects of Salinity on the Dissolution of Phlogopite.** Within 1 h after 102 atm CO<sub>2</sub> was introduced, the in situ pH of the scCO<sub>2</sub>–H<sub>2</sub>O(l)–phlogopite system at 368 K dropped from 6.15 ± 0.05 to 3.19 ± 0.05, and it remained in that range during the following 159 h. This pH was slightly higher than that in the scCO<sub>2</sub>–1 M NaCl–phlogopite system, where the stabilized pH was 3.08 ± 0.05.<sup>6</sup>

The kinetics of phlogopite dissolution in water and 1 M NaCl were significantly different, especially at the later reaction time (Figure 2). In NaCl solution, the concentrations of Mg, Al, Si, and K increased almost linearly over 159 h, suggesting that the reaction rate remained constant, whereas in water, the reaction rate started to decrease after 70 h. To determine whether the dissolution of phlogopite was congruent, we normalized the concentrations of Mg, Al, Si, and K, based on phlogopite stoichiometry [KMg<sub>2.87</sub>Si<sub>3.07</sub>Al<sub>1.23</sub>O<sub>10</sub>(F,OH)<sub>2</sub>]. The results (Figure 2e,f) suggest that the dissolution of phlogopite was incongruent in both water and NaCl solutions. Preferential dissolution of elements was observed in this order: K > Mg ≈ Si > Al in water, K > Mg ≈ Si ≈ Al before 70 h in NaCl solution, and K > Mg ≈ Si > Al after 70 h in NaCl solution. Potassium dissolved preferentially from the interlayers in both water and NaCl solution, but the high concentration of Na<sup>+</sup> in 1 M NaCl solution facilitated ion exchange between Na<sup>+</sup> and K<sup>+</sup> in phlogopite interlayers<sup>15</sup> and thus made the dissolved K<sup>+</sup> concentration around 30 times higher than that in water at 159 h. The different dissolution patterns of phlogopite in pure water and NaCl solution suggest that salinity does influence the reaction mechanisms.

So far, most studies on the effect of salinity on mineral dissolution have been conducted without the presence of scCO<sub>2</sub>. Kuwahara and Aoki reported that phlogopite dissolved preferentially in the order of K > Mg ≈ Al > Si within 96 h in 0.01 M HCl + 0.1 M NaCl solution at elevated temperature (323–393 K).<sup>15</sup> Another study of phlogopite in water at 1 atm CO<sub>2</sub> and room temperature reported that Mg dissolution was preferred over Si dissolution,<sup>16</sup> while the present work shows similar dissolution rates of Mg and Si. The different behavior of phlogopite at low CO<sub>2</sub> pressure (1 atm) or in acid solution, and under GCS conditions (this work), suggests that the reaction mechanisms between rock minerals and CO<sub>2</sub>-saturated saline water could differ from changes in ambient conditions. Therefore, further investigations are needed to resolve the reaction pathway differences.

**Effects of Salinity on the Morphological Changes of Phlogopite Surfaces.** AFM analysis of phlogopite (Figure 3) showed that solution salinity influenced the size of dissolution pits and the location, size, and shape of secondary mineral phases. For all the samples in water (low salinity) and in 1 M NaCl (high salinity), dissolution pits were the predominant surface feature, which is consistent with our aqueous solution analysis results (Figure 2) that indicate the dissolution of species from phlogopite surface. However, in 1 M NaCl solution, the dissolution pits were much deeper than those in water at the same reaction time.

The different behavior of phlogopite dissolution in low and high salinity solutions can be explained by the layered structure of phlogopite as a 2:1 sheet silicate. The ion-exchange between aqueous Na<sup>+</sup> and phlogopite interlayer K<sup>+</sup> caused a swelling of the phlogopite (Figure 3D).<sup>17</sup> Thus, an increase in the interlayer distance allowed more interlayer surfaces to come in contact with the aqueous solution, increasing the reactive surface area, and consequently enhancing phlogopite dissolution. Evidence for this explanation was obtained from the change of phlogopite layer thicknesses after reaction (Figure 3C–E). The layer thicknesses in NaCl solution were in the range of 1.20–1.60 nm. The nearer the layer is to the surface, the greater the layer thickness, suggesting that the swelling is more pronounced for surface layers than inner layers. Furthermore, in NaCl solution, the dissolution pits that formed on the interlayer surfaces, as observed by Aldushin et al.,<sup>18</sup> could serve as defects; thus, when the upper layer was penetrated and the lower layer was exposed to the bulk acid solution, the pits facilitated the dissolution of the lower layer. In water, however, the layer depth was generally in the range of 1.0–1.2 nm (Figure 3E), which was only slightly larger than unaltered phlogopite (1 nm).<sup>18</sup> The different layer thicknesses in water and NaCl solution also indicate that layer expansion was not a manifestation of pulling pressure off the sample during CO<sub>2</sub> release at the end of an experiment, because all experiments followed the same procedures.

The formation of secondary mineral phases was observed in both water and NaCl solutions. However, the morphology of new solids in the two reaction systems differed in several ways. First, the new solid phases in water appeared after only 3 h, which was faster than in NaCl solution (5 h, Figure 3A1,B1). This phenomenon could be explained by the low aqueous species activity in NaCl solution due to the high ionic strength. Thus, as the dissolved species accumulated in the aqueous solution, supersaturation may first occur in water, although the concentration in NaCl solution may be higher. Thus, precipitation in water could occur earlier than in NaCl solution. Our thermodynamic calculations for the activity of the dissolved species confirmed that the activities of Mg<sup>2+</sup> and Al<sup>3+</sup> in water were higher than in NaCl solution through the entire reaction period, while K<sup>+</sup> activity in water was higher in NaCl solution due to ion-exchange (Figure S2, Supporting Information).

Second, the location of the new solid was different: in 1 M NaCl solution, the new particles first appeared near the edges of dissolution pits, whereas in water, nanoparticles formed on both terraces and pit edges (Figure 3A1,B1). This effect of salinity can be related to the system's supersaturation ratio of secondary minerals. In water, the higher supersaturation ratio of the potential secondary mineral phase(s) on phlogopite surfaces makes nucleation on terraces the predominant process, compared with that at steps.<sup>19</sup> In 1 M NaCl, the lower supersaturation favored nucleation near steps or kinks to compensate for the free energy barrier. Consequently, we observed that in NaCl solution, the precipitates were initially located near the dissolution pit edges, whereas in water, early stage precipitation formed randomly on the phlogopite surface (A2 in Figure 3). In addition, the changes of surface tension in high salinity solution could also affect the location of secondary mineral phases.

Third, the growth and aggregation of new particles were different: as the reaction time increased, new particles in NaCl solution grew and started to aggregate after 22 h, whereas in water, the particle size did not increase significantly before 70 h. At 3, 8, 22, and 43 h in water, the average particle heights

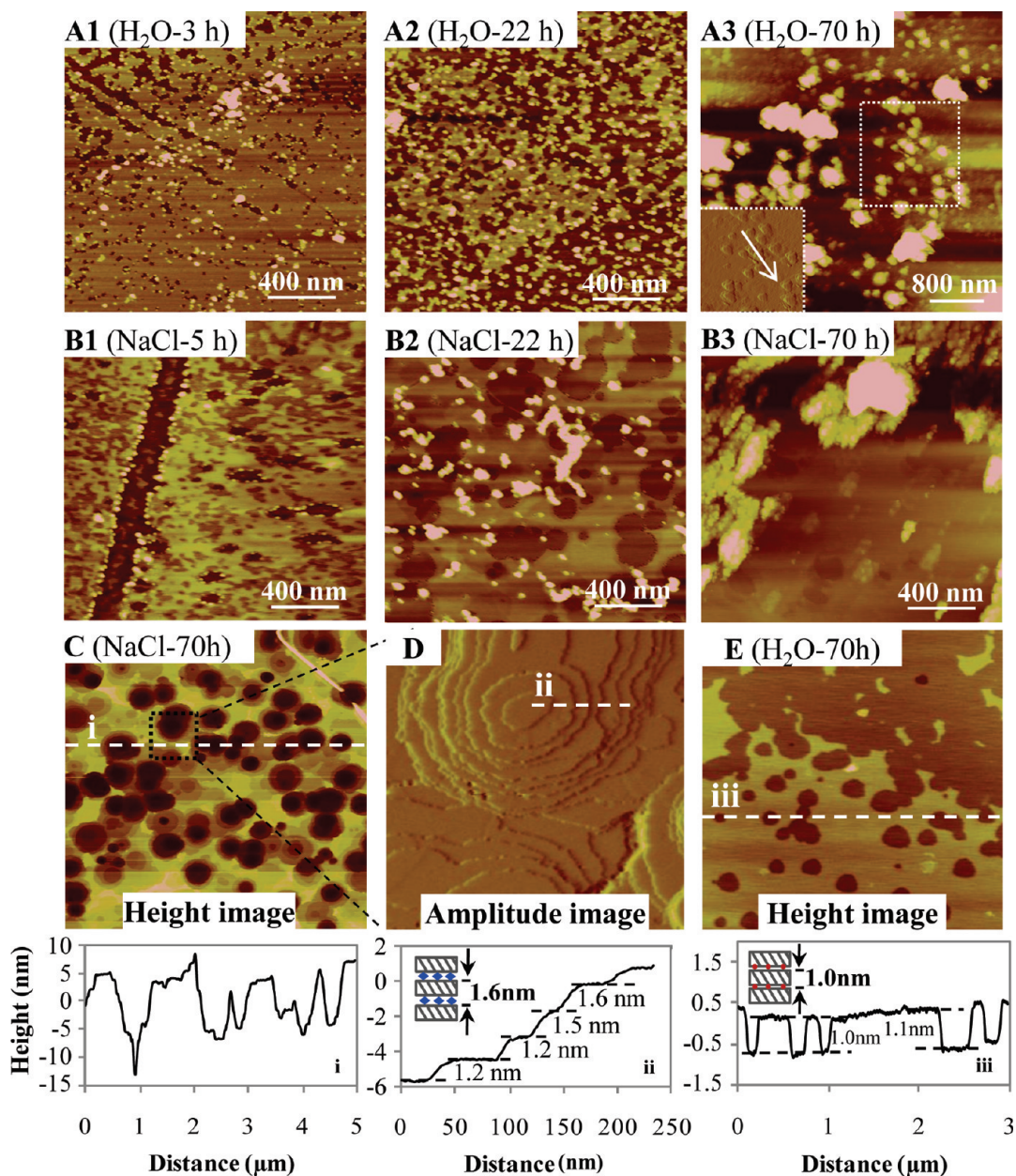


**Figure 3.** Formation of secondary mineral phases (A1–3 and B1–3) and dissolution pits (C, D, and E) on the phlogopite surface after reaction in water and in 1 M NaCl at different times. The inset in A3 is an amplitude image for the area framed with the dashed line, and the white arrow indicates the alignment of the triangular apices. Image D is enlarged from the small area of image C. The height cross-sections under images C, D, and E correspond to the white dotted lines in the images. The cartoons at the left corner of D and E height cross-section panels schematically illustrate the phlogopite layer swelling. The blue diamonds and red dots correspond to the ion exchanged  $\text{Na}^+$  and  $\text{K}^+$  in the original layer, respectively.

were  $3.1 \pm 1.0$ ,  $3.0 \pm 0.9$ ,  $3.6 \pm 0.6$ , and  $3.1 \pm 0.5$  nm (based on measurements of 30 particles, uncertainties are the standard deviation), respectively, and the horizontal dimensions (in the longest direction) were  $29.4 \pm 8.1$ ,  $37.9 \pm 6.6$ ,  $34.8 \pm 8.4$ , and  $30.1 \pm 6.4$  nm, respectively. This result suggests that, nucleation, rather than growth, was the dominated process at the early stage of particle development in low salinity solution.<sup>20</sup> Only after 70 h, particle aggregation was observed in water (A3 in Figure 3). The early development of aggregation in NaCl solutions might be the result of the compressed electric double layer.<sup>20</sup> Furthermore, after 70 h, while the irregular shaped precipitates (amorphous phases) formed at the same surface without any general trend (Figure 3A3), some triangular particles appeared on the surface

and lined up in one direction. This observation suggests that some secondary mineral phases become more crystallized and grow heteroepitaxially (i.e., following the substrate's crystal structure) compared with those particles initially formed.

**Effects of the Extent of Water on  $\text{scCO}_2$ -Induced Morphological Changes of Phlogopite.** When phlogopite contacted  $\text{scCO}_2\text{-H}_2\text{O}(\text{g})$ , the formation of dissolution pits and secondary mineral phases resulted in significant changes of surface morphology (Figure 4). Similar to the condition where phlogopite was in contact with  $\text{scCO}_2\text{-H}_2\text{O}(\text{l})$ , dissolution pits were the predominant surface feature in the  $\text{scCO}_2\text{-H}_2\text{O}(\text{g})$  system. However, the dissolution pit depths in  $\text{scCO}_2\text{-H}_2\text{O}(\text{g})$  were generally in the range of 1.2–2.0 nm, and a few reached as deep

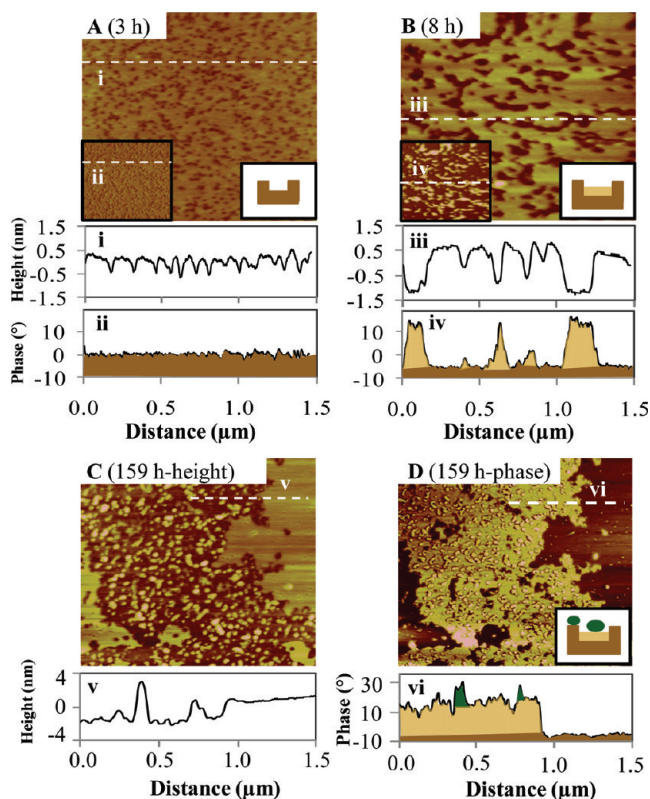


**Figure 4.** Formation of dissolution pits and secondary mineral phases on phlogopite surfaces after reaction with  $\text{scCO}_2\text{-H}_2\text{O}(\text{g})$  at 102 atm of  $\text{CO}_2$  and 368 K for different times. Image A, B, and C are in height mode. The insets in the left bottom corner of A and B are the corresponding phase mode images for A and B; image D is the corresponding phase mode image for C. The height cross-sections (i, iii, and v) and the phase shift cross-sections (ii, iv, and vi) under the images correspond to the white dotted line in the AFM images. The phase mode can detect variations in chemical and mechanical properties such as friction and adhesion. The cartoons at the right bottom corner of A, B, and C schematically illustrate the dissolution pits and the position of secondary mineral phases (with yellow and green color). The brown color corresponds to unaltered phlogopite.

as 5 nm (data not shown). Those pits are deeper than in the  $\text{scCO}_2\text{-H}_2\text{O}(\text{l})$  system, suggesting that the  $\text{scCO}_2\text{-H}_2\text{O}(\text{g})$  system is more reactive than the  $\text{scCO}_2\text{-H}_2\text{O}(\text{l})$  system.

The formation of different mineral phases can be detected based on differences in contrasts in AFM phase image. AFM analysis showed that the secondary phase formed after only 8 h and were first observed on the bottom of dissolution pits (Figure 4B). After a longer reaction time (159 h), the secondary phase covered larger surface areas (Figure 4C,D), which is evident by the similar phase shift values ( $15\text{--}20^\circ$ ) for the new phases at pit bottom at 8 and 159 h. This new layer (or surface coating) could consist of a thin film of the newly formed phase or a leached layer as a result of incongruent dissolution. At the same time, isolated nanoscale precipitates also formed on both the unaltered surface and the new layer (Figure 4C and 4D). The nanoparticles were different from the surface coating, indicated by the higher phase shift values (Figure 4 cartoons and the phase cross-section panels).

McGrail et al. stated that in a  $\text{scCO}_2\text{-H}_2\text{O}(\text{g})$  system, water is present as a gas, and there is no liquid phase.<sup>13</sup> However, Lin et al. proposed that a thin water film may be adsorbed on mineral

surfaces, and because  $\text{CO}_2$  diffused into this thin water film more easily than the bulk water in the  $\text{scCO}_2\text{-H}_2\text{O}(\text{l})$  system, the  $\text{scCO}_2\text{-H}_2\text{O}(\text{g})$  system should have higher reactivity.<sup>21</sup> Our result suggests that a thin water layer is indeed present, and it can accommodate the dissolved species from phlogopite, as evident by the formation of dissolution pits, new phase layers, and nanoparticles.

**Identification of the Secondary Mineral Phases.** DRIFTS spectra of powdered samples (Figure 5A) showed peaks in the  $900\text{--}1200\text{ cm}^{-1}$  range, attributed to Si–O bands.<sup>22</sup> For the  $\text{scCO}_2\text{-H}_2\text{O}(\text{l})\text{-phlogopite}$  system, the peak area was 2.2 times larger than that of unreacted phlogopite and 1.3 times larger than that of  $\text{scCO}_2\text{-NaCl-phlogopite}$ . The area of the small peak at  $815\text{ cm}^{-1}$ , attributed to Al–O bands,<sup>22</sup> was 1.4 times larger for  $\text{scCO}_2\text{-H}_2\text{O}(\text{l})\text{-phlogopite}$  than for unreacted phlogopite and 1.2 times larger than for  $\text{scCO}_2\text{-NaCl-phlogopite}$ . Therefore, in water, more secondary mineral phases containing Si–O bands and, to a lesser extent, Al–O bands formed than in NaCl solution. In the  $\text{scCO}_2\text{-H}_2\text{O}(\text{g})$  system, after 159 h reaction, the Si–O bands only slightly increased, compared with unreacted phlogopite, suggesting that the reaction is limited by the extent of water on the phlogopite surface.

The HR-TEM analysis showed that a significant amount of an amorphous material, indicated by the electron diffraction pattern, was present in the  $\text{scCO}_2\text{-H}_2\text{O}(\text{l})\text{-phlogopite}$  system (Figure 5B). Combining the result from DRIFTS (significant amount of Si–O bands were formed after reaction) and a previous study providing the morphology of synthesized amorphous silica,<sup>23</sup> we concluded that the particles in Figure 5B are likely to be amorphous silica. Kaolinite [ $\text{Al}_2\text{Si}_2\text{O}_5(\text{OH})_4$ ], diaspore [ $\alpha\text{-AlO}(\text{OH})$ ], boehmite [ $\gamma\text{-AlO}(\text{OH})$ ], and gibbsite [ $\text{Al}(\text{OH})_3$ ] were identified with HR-TEM based on the electron diffraction patterns and their morphologies, but their abundance was much less than that of amorphous silica, which is consistent with our findings in DRIFTS. These crystallized minerals are likely to correspond to the facet structures that we found on AFM images (Figure 3A3). In our previous study, we demonstrated that amorphous silica (major) and kaolinite were the products of a  $\text{scCO}_2\text{-NaCl-phlogopite}$  system.<sup>6</sup> Compared with a 1 M NaCl system, more amorphous silica and aluminum-containing minerals were observed on the HR-TEM grids for the  $\text{scCO}_2\text{-H}_2\text{O}(\text{l})\text{-phlogopite}$  system, suggesting that low salinity allowed more secondary mineral phases to remain in the bulk solution. Although synchrotron-based HR-XRD analysis was also conducted, no new peaks other than phlogopite were identified. This result suggests that either the amount of crystalline minerals was too small to be detected or that the main secondary mineral phase was amorphous.

**Environmental Implications.** Salinity, an important environmental factor, was found to influence both phlogopite dissolution and secondary mineral formation under GCS conditions. In this work we demonstrated that low salinity solutions can enhance the formation of nanoscale secondary mineral phases. Although the amount of new particles was not significant, compared with the preexisting minerals, it may significantly change the permeability of the reservoir rocks or caprocks by clogging the nanoscale pore throats.<sup>3,6</sup>

Furthermore, we reported that  $\text{scCO}_2$ -induced reactions occur not only with rocks in contact with acidified saline water but also with those in contact with  $\text{scCO}_2\text{-H}_2\text{O}(\text{g})$ . The formation of spreading secondary minerals, which are less soluble than the original rock, will change the chemical and physical properties of rocks that contain clay minerals. First, as a surface coating, they will decrease the reactivities of reservoir rocks, as Nugent et al.

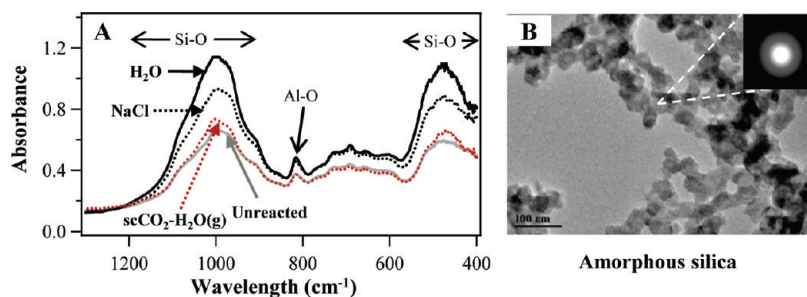


**Figure 5.** DRIFTS (A) and TEM (B) results for secondary mineral phase identification. DRIFTS spectra are for phlogopite powder before and after reacting in  $\text{scCO}_2\text{-H}_2\text{O(l)}$ ,  $\text{scCO}_2\text{-1 M NaCl}$  solution, and  $\text{scCO}_2\text{-H}_2\text{O(g)}$  under 102 atm and 368 K, respectively for 159 h. The TEM image is for amorphous silica particles in the supernatant of powdered phlogopite after reaction with  $\text{CO}_2$  in water for 159 h. The inset in B is the electron diffraction pattern collected from the area pointed by the dashed lines.

suggested.<sup>24</sup> So far, all the modeling work assumes that the minerals dissolve with constant reaction rates; however, this work suggests that rocks initially in contact with  $\text{scCO}_2\text{-H}_2\text{O(g)}$ , and later in contact with saline water due to the dissolution of  $\text{scCO}_2$ , will have different reactivities from unaltered minerals (regime A  $\rightarrow$  regime B in Figure 1). Second, the formation of a surface coating will change the wettability of reservoir rocks and caprocks and consequently influence the transport of  $\text{scCO}_2$ . Under our experimental conditions, formation of surface coatings on phlogopite occurred less than a week after  $\text{CO}_2$  injection. While  $\text{scCO}_2$ 's transport in the formation rock can be hindered by the formation of surface coatings, the coating can also beneficially contribute to sealing the caprock at the host rock/cap rock interfaces. Therefore, the surface coatings or nanoparticle formation can be an important consideration in designing a safer GCS site.

## ASSOCIATED CONTENT

**Supporting Information.** Descriptions of the experimental methods, three figures (experimental setup, activity of metal ions in different salinity solutions, and HR-TEM results), and two tables (experimental parameters and the result from  $\text{N}_2$  control experiments) are available free of charge via the Internet at <http://pubs.acs.org>.

## AUTHOR INFORMATION

### Corresponding Author

\*Phone: (314) 935-4539; fax: (314) 935-7211; e-mail: [ysjun@seas.wustl.edu](mailto:ysjun@seas.wustl.edu); internet: <http://encl.engineering.wustl.edu/>.

## ACKNOWLEDGMENT

This work is supported by the Consortium for Clean Coal Utilization, and Y.S.J. was partially supported by the Office of Basic Energy Sciences of the U.S. Department of Energy, in association with the Energy Research Frontier Center of Berkeley Lab, under Contract No. DE-AC02-05CH11231.

## REFERENCES

- (1) Bachu, S. Sequestration of  $\text{CO}_2$  in geological media: criteria and approach for site selection in response to climate change. *Energy Convers. Manage.* **2000**, *41* (9), 953–970.
- (2) IPCC. *Special Report on Carbon Dioxide Capture and Storage*; Working Group III of the Intergovernmental Panel on Climate Change; Cambridge University Press: Cambridge, U.K., 2005.

- (3) Gaus, I. Role and impact of  $\text{CO}_2$ -rock interactions during  $\text{CO}_2$  storage in sedimentary rocks. *Int. J. Greenhouse Gas Control* **2010**, *4* (1), 73–89.

- (4) White, C. M.; Strazisar, B. R.; Granite, E. J.; Hoffman, J. S.; Pennline, H. W. Separation and capture of  $\text{CO}_2$  from large stationary sources and sequestration in geological formations-coalbeds and deep saline aquifers. *J. Air Waste Manage. Assoc.* **2003**, *53*, 645–715.

- (5) Luquot, L.; Gouze, P. Experimental determination of porosity and permeability changes induced by injection of  $\text{CO}_2$  into carbonate rocks. *Chem. Geol.* **2009**, *265* (1–2), 148–159.

- (6) Shao, H.; Ray, J. R.; Jun, Y.-S. Dissolution and precipitation of clay minerals under geologic  $\text{CO}_2$  sequestration conditions:  $\text{CO}_2$ -brine-phlogopite interactions. *Environ. Sci. Technol.* **2010**, *44* (15), 5999–6005.

- (7) Olsen, A. A. Forsterite dissolution kinetics: applications and implications for chemical weathering. Ph.D. thesis, Virginia Polytechnic Institute and State University, Blacksburg, VA, 2007.

- (8) Keller, S. J. *Analyses of subsurface brines of Indiana*; Department of Natural Resources: Bloomington, IN, 1983.

- (9) Kharaka, Y. K.; Hanor, J. S. Deep fluids in the continents: 1. sedimentary basins. In *Surface and Ground Water, Weathering and Soils, Treatise on Geochemistry*; Drever, J. I., Ed.; 2007; Vol. 5, pp 1–48.

- (10) Dove, P. M.; Crerar, D. A. Kinetics of quartz dissolution in electrolyte solutions using a hydrothermal mixed flow reactor. *Geochim. Cosmochim. Acta* **1990**, *54*, 955–969.

- (11) Stillings, L. L.; Brantley, S. L. Feldspar dissolution at 25°C and pH 3: Reaction stoichiometry and the effect of cations. *Geochim. Cosmochim. Acta* **1995**, *59* (8), 1483–1496.

- (12) Spycher, N.; Pruess, K.; Ennis-King, J.  $\text{CO}_2\text{-H}_2\text{O}$  Mixtures in the Geological Sequestration of  $\text{CO}_2$ . I. Assessment and Calculation of Mutual Solubilities from 12 to 100 °C and up to 600 bar. *Geochim. Cosmochim. Acta* **2003**, *67*, 3015–3031.

- (13) McGrail, B. P.; Schaef, H. T.; Glezakou, V. A.; Dang, L. X.; Owen, A. T. Water reactivity in the liquid and supercritical  $\text{CO}_2$  phase: has half of the story been neglected?. *Energy Procedia* **2009**, *1* (1), 3415–3419.

- (14) Guggenheim, S.; Martin, R. T. Definition of clay and clay mineral: joint report of the AIPEA nomenclature and CMS nomenclature committees. *Clays Clay Miner.* **1995**, *43* (2), 255–256.

- (15) Kuwahara, Y.; Aoki, Y. Dissolution process of phlogopite in acid solutions. *Clays Clay Miner.* **1995**, *43* (1), 39–50.

- (16) Lin, F.; Clemency, C. V. Dissolution kinetics of phlogopite. I. Closed system. *Clays Clay Miner.* **1981**, *29*, 101–106.

- (17) Newman, A. C. D. The synergistic effect of hydrogen ions on the cation exchange of potassium in micas. *Clay Miner.* **1970**, *8*, 361–373.

- (18) Aldushin, K.; Jordan, G.; Schmah, W. W. Basal plane reactivity of phyllosilicates studied in situ by hydrothermal atomic force microscopy (HAFM). *Geochim. Cosmochim. Acta* **2006**, *70* (17), 4380–4391.

- (19) De Yoreo, J. J.; Vekilov, P. G. Principles of crystal nucleation and growth. *Rev. Mineral. Geochem.* **2003**, *54*, 57–93.

(20) Jun, Y.-S.; Lee, B.; Waychunas, G. A. *In situ* observations of nanoparticle early development kinetics at mineral–water interfaces. *Environ. Sci. Technol.* **2010**, *44* (21), 8182–8189.

(21) Lin, H.; Fujii, T.; Takisawa, R.; Takahashi, T.; Hashida, T. Experimental evaluation of interactions in supercritical CO<sub>2</sub>/water/rock minerals system under geologic CO<sub>2</sub> sequestration conditions. *J. Mater. Sci.* **2008**, *43*, 2307–2315.

(22) Farmer, V. C. The layer silicate. In *The Infrared Spectra of Minerals*; Farmer, V. C., Ed.; Mineralogical Society: London, 1974.

(23) Xu, Y.-M.; Qi, J.; He, D.-M.; Wang, D.-M.; Chen, H.-Y.; Guan, J.; Zhang, Q.-M. Preparation of amorphous silica from oil shale residue and surface modification by silane coupling agent. *Oil Shale* **2010**, *27* (1), 37–46.

(24) Nugent, M. A.; Brantley, S. L.; Pantano, C. G.; Maurice, P. A. The influence of natural mineral coatings on feldspar weathering. *Nature* **1998**, *395*, 588–591.